

## Two-dimensional and three-dimensional numerical analysis of high-rise slope stability in an open-pit mine

### *Análise numérica bidimensional e tridimensional de estabilidade de talude de grande altura em mina a céu aberto*

Alessandro Fidelis dos Santos<sup>1</sup>, Thiago Bomjardim Porto<sup>2</sup>, Thiago Cruz Bretas<sup>3</sup>

<sup>1</sup> Federal Center for Technological Education of Minas Gerais, Graduate Program in Mining Engineering, Araxá/MG, Brazil. Email: mine.tpo@gmail.com

**ORCID:** <https://orcid.org/0009-0007-3661-0635>

<sup>2</sup> Federal Center for Technological Education of Minas Gerais, Graduate Program in Mining Engineering, Araxá/MG, Brazil. Email: thiago.porto@cefetmg.br

**ORCID:** <https://orcid.org/0000-0002-3355-0477>

<sup>3</sup> Federal Center for Technological Education of Minas Gerais, Graduate Program in Mining Engineering, Araxá/MG, Brazil. Email: tbretas@gmail.com

**ORCID:** <https://orcid.org/0000-0002-2970-3477>

**Abstract:** The slope stability analyzes most used in geotechnical engineering practice are in two dimensions. However, the evaluation in three dimensions tends to be more rigorous, and more justifiable to represent the real condition of the geometry of the unstable terrain mass. Thus, advances in the theory of three-dimensional stability analysis, the increase in the processing power of personal computers and the development of more robust software packages, have allowed engineers, designers, and researchers to present these analyzes in a more assertive and pragmatic way. In this way, the article develops the analysis of the two-dimensional and three-dimensional slope stability of a pit of an open-pit mine located within the Mineral Complex of Patrocínio-MG, with height in the order of 375m, with banks of 10m, evaluating the consistency of the database available and, in sequence, the results obtained. The geology of the region is characterized by an economic alkaline deposit of phosphate that occurs in the central area located entirely within the Salitre I dome. To sectorize the critical section of the slope of the pit of this research, the automatic search tool of the Slide3 Software from the company Rocscience® was used.

**Keywords:** 2D and 3D stability analysis; Limit equilibrium; Automatic search; Critical section; Open pit mine.

**Resumo:** As análises de estabilidade de talude mais comumente utilizadas na prática da engenharia geotécnica são em duas dimensões. Porém, a avaliação em três dimensões tende a ser mais rigorosa, e mais justificável para representar a condição real de geometria da massa do terreno instável. Assim os avanços na teoria da análise de estabilidade tridimensional, o aumento do poder de processamento dos computadores pessoais e o desenvolvimento de pacotes de software mais robustos, tem permitido que os engenheiros, projetistas e pesquisadores apresentassem estas análises de maneira mais assertiva e pragmática. Desta forma, o artigo desenvolve a análise de estabilidade de talude bidimensional e tridimensional de uma cava de uma mina a céu aberto situada dentro do Complexo Mineral de Patrocínio-MG, com altura na ordem de 375m, com bancos de 10m, avaliando a consistência da base de dados disponível e, na sequência, os resultados obtidos. A geologia da região é caracterizada por depósito econômico alcalino de fosfato que ocorre na área central localizada integralmente dentro do domo Salitre I. Para setorização do trecho crítico do talude da cava desta pesquisa, utilizou-se a ferramenta de busca automática do Software Slide3 da empresa Rocscience®.

**Palavras-chave:** Análises de estabilidade 2D e 3D; Equilíbrio-limite; Busca automática; Trecho crítico; Mina a céu aberto.

## 1. Introduction

To enhance the extraction of mineral resources, the slopes of open-pit mines have reached great heights and inclinations. However, it should be noted that the greater the slope slope, the more unstable they become and consequently the greater the associated risks (Oliveira, 2020). Thus, there is a growing need for methodologies that ensure that these excavations are safe and cost-effective simultaneously (Capelli, 2018).

Among the main methods of geotechnical validation of the operational pit and final mining pit is the evaluation of slope stability, highlighting the limit equilibrium methods and stress-strain numerical analysis methods. In recent decades, deterministic methods have been used to predict slope safety, both in two- and three-dimensional models (Costa, 2005).

2D methods are the traditional forms in slope stability analysis due to their simplicity, however, such methods are based on different simplifications, usually in reducing the number of unknowns, to reduce the real three-dimensional problem in a two-dimensional model, making the accuracy reduced, (Antocheviz, 2018). Anagnosti (1969) shows that the number of assumptions required to satisfy all equilibrium equations in 3D is four times greater than in a 2D analysis and that, the comparison with some analyses, assuming slices in 2D, reveals that the factor of safety can increase by up to 50% using 3D methods. One of the challenges in slope stability analysis is to use the results of three-dimensional analysis in decision-making. Currently, decision-makers often choose to use the results of 2D analysis to the detriment of 3D analysis, as two-dimensional analyses are usually conservative (Bretas, 2020).

To determine the Safety Factor (FS) of a pit slope, it is necessary to establish premises for the physical-mathematical problem to have a deterministic solution. The most recent theoretical models enable the solution based on iterative calculation. The greater the number of problem unknowns, the greater the computational requirement to solve the geotechnical problem, both for three-dimensional analysis methods as well as 2D methods. To optimize the problem, it is common to decrease the number of unknowns, or, alternatively, to increase the number of equations (Albataineh, 2006). Zhou and Cheng (2006) proposed a rigorous method where it satisfies all equilibrium conditions (forces and moments) and can perform an automatic search of the critical rupture surface and determine the safety factor for three-dimensional slopes or landslides with a known and arbitrarily shaped slip surface.

The availability of computer programs for three-dimensional stability analysis by equilibrium limit, as well as the availability of computers with increasing processing capacity, are important elements to stimulate the use of 3D modeling in comparison with 2D stability analyses, given the gain in economy in the enterprise, in terms of cost-benefit ratio. The use of numerical methods is a powerful tool in the elaboration of geometric designs of open-pit pits, allowing the creation of rigorous models, not possible with traditional limit equilibrium methods (Antocheviz, 2018).

Three-dimensional stability analysis software by limit equilibrium has become popular among geotechnicians since the 2000s, as its use was restricted to large research centers (academia). That said, this work is justified by the fact that it analyzes a real problem, which is the sectorization of the critical section of the final slope of the pit of this research, through 3D analysis and evaluation of the consistency of the results obtained in a more rigorous way, constituting an important contribution to the mining company's decision-making.

In this way, geotechnical studies applied to stability analysis considering pit slopes are extremely important and essential for mining, as they seek to ensure safety in operations, sustainable advancement, and prediction of enterprises. For mining pits, global slope failures are usually immensely costly for the entrepreneur (Bretas, 2020).

## 2. 2D and 3D Boundary Balance Methods

The methods currently used in slope stability analysis are based on the hypothesis that the geotechnical massifs are in equilibrium and behave as a rigid-plastic body on the verge of landslide, thus simply analyzing the equations for the limit situation, thus being called limit equilibrium methods (Silva, 2011).

Aguilera (2009) mentions that most methods of limit equilibrium analysis have in common the comparison of the forces or resistant moments with the ones acting on a given slip surface. All methods assume that in the event of failure, the acting and resistant forces/moments are equal along a fault surface and equivalent to a safety factor (FS) of 1.0 (one unit). According to Cheng and Lau (2008), the safety factor (FS) can be defined as the ratio between the resisting forces (ER) and the stressing forces (ES) along the rupture surface, or the ratio between the resistant shear stress and the mobilized shear stress on the critical surface, as shown in (Equation 1).  $(\tau_f) \tau_{mob}$

$$FS = \frac{E_R}{E_s} = \frac{\tau_f}{\tau_{mob}} \quad (1)$$

The available shear strength of the soil to ensure the balance of the sliding body is defined as per (Equation 2).  $(\tau_f)$

$$\tau_f = c' + (\sigma_n - u) \tan \varphi \quad (2)$$

Where:

$c'$  it's cohesion in terms of effective tensions,

$\varphi$  is the angle of internal friction of the material in terms of effective stresses,  
 $\sigma_n$  is the total normal voltage,  
 $u$  it's porooppresion.

In 2D limit equilibrium methods, the rupture surface is discretized into a series of slices. Figure 1A shows the division of a soil mass into slices, and Figure 1B shows a generic  $i$  slice, with the forces acting on it, where  $W_i$  is the weight of the slice;  $N'_i$  a resulting from the normal effective stresses at the base of the slice;  $U_i$  the result of pore oppresion at the base of the slice;  $T_i$  the result of the tangential stresses mobilized at the base of the slice;  $E_i$  and  $X_i$  the normal and tangential components, respectively, of the interaction forces between the slices on the left face;  $E_{i+1}$  and  $X_{i+1}$  are the components of the interaction forces between the slices on the right face and  $S_c$  loads.

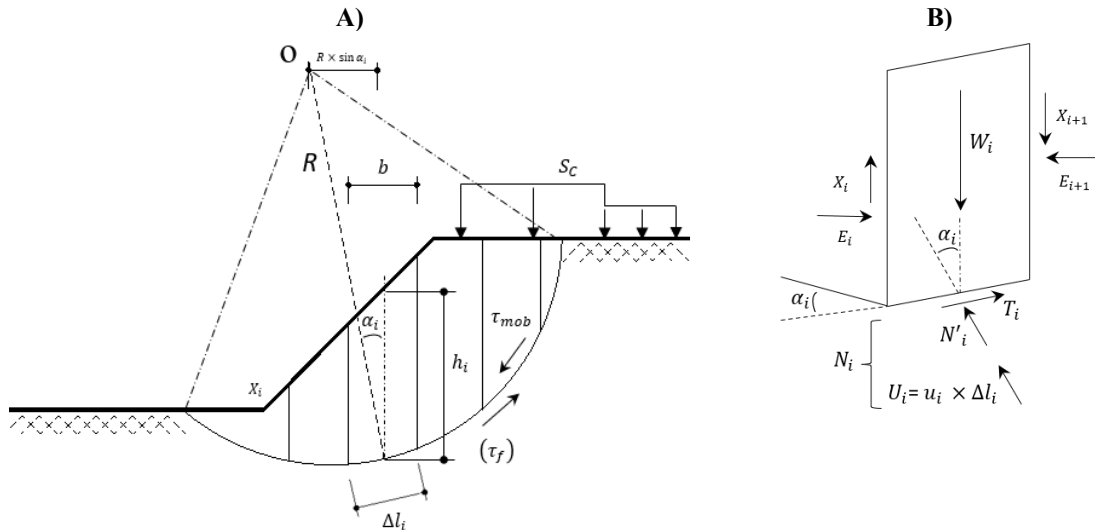


Figure 1 – (A) Potentially unstable soil mass divided into slices. (B) Representation of the  $i$ -th slice and the forces acting on it.  
Source: Authors (2023).

According to the slice method, the soil mass above the assumed rupture surface is divided into vertical slices, the amount of which depends on the geometry of the slope and the stratigraphy of the geotechnical massif. The rupture surfaces evaluated can be either circular or arbitrary in shape (non-circular).

Thus, for the method of Fellenius (1936) both the normal forces and the shear forces on the sides of the slices are neglected, and the safety factor (FS) is expressed in terms of momentum and is defined by Equation 3.

$$FS = \frac{\sum c' \cdot \left( \frac{b}{\cos \alpha} \right) + (W \cdot \cos \alpha - u \cdot \left( \frac{b}{\cos \alpha} \right) \cdot \tan \varphi}{\sum W \cdot \sin \alpha} \quad (3)$$

This procedure is repeated for various positions on the rupture surface. The critical safety factor corresponds to the one with the lowest value found for FS.

Many of the existing 3D methods are direct extensions of 2D slope stability methods. Gens et al (1988) developed the Swedish Circle method to establish a new 3D method. The method of (Hovland, 1977) together with the method of (Ugai, 1988) and (Zheng, 2009) were developed as extensions of the common method of slicing. The simplified method of (Bishop, 1955) served as the basis for the 3D methods of (Hung, 1987), (Ugai, 1988), (Hung et al. 1989) and (Cheng et yip, 2007). Ugai, (1988), (Hung et al., 1989), (Yamagami and Jiang, 1997), (Cheng and Yip, 2007) proposed different 3D methods, developing the (Junbu, 1973) method. The extension of the method from (Spencer, 1967) provided several 3D methods from (Chen, 1981), (Chen and Chameau, 1982), (Ugai, 1988), (Cheng et al. 2003), and (Jiang and Yamagami, 2004). The 3D boundary equilibrium method of (Cheng and Yip, 2007) was established as an extension of the method of (Morgenstern and Price, 1965). The 3D methods of (Lam and Fredlund, 1993) and (Huang et al. 2002) are an extension of the generalized slice method. By extension of the 2D circular arc method, (Baligh and Azzouz, 1975), (Azzouz and Baligh, 1978) and (Cavounidis and Kalogeropoulos, 1992) presented 3D extensions.

To convert the slice methods to three-dimensional slopes, the slices were transformed into columns, adding a third dimension (Kalehjari and Ali, 2013). Thus, slope stability analysis by three-dimensional limit equilibrium is simple in concept, and directly analogous to two-dimensional methods (Rocscience, 2022), namely:

- In 2D, a sliding mass is discretized into vertical slices;
- In 3D, the evaluated mass is discretized into columns, with a square cross-section, while in a usual two-dimensional modeling, the mass is partitioned into slices.

Initial models proposed for 3D limit equilibrium stability analysis were subject to several constraints, such as:

- Assume a direction of slippage;
- Assume a plane of symmetry;
- Balance transversal forces and/or unsatisfied moments;
- Require local coordinate system;
- Require simplified wedge search methods (such as spherical and planar).

Huang et al. (2002) proposed considerable improvements in three-dimensional stability analyses, as shown in Figure 2A and Figure 2B later extended by (Cheng and Yip, 2007) and used by the Slide3 *Limit Equilibrium Analysis for Slopes* (Rocscience®) as:

- Equilibrium of forces and moments in two orthogonal directions;
- Efficient solver for 3D equilibrium equations;
- Any failure criterion may be used (not limited to Mohr-Coulomb);
- Rapid search methods for general 3D sliding surfaces;
- Geometric modeling and data interpretation capabilities.

The weight of the soil mass and the vertical loads are considered to act in the center of each column as simplification (Cheng and Lau, 2008).

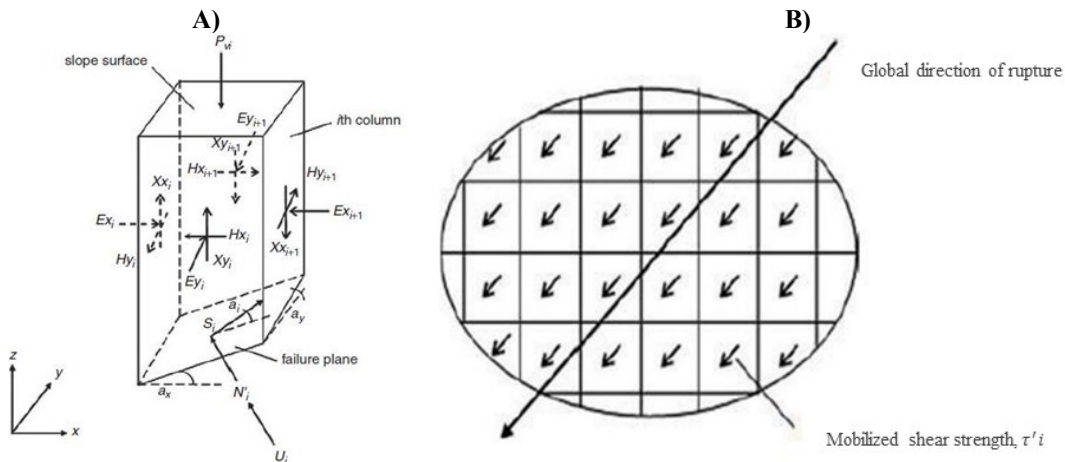


Figure 2 – (A) External and internal forces acting on a typical column. (B) Single slip direction for all columns – Plan view.

Source: Chen and Lau (2008).

Where:

There is the slope of the base of the column projected to the x-y plane;

$a_x, a_y$  are the slopes of the base of the column in the x and y directions measured from the center of each column;

$Ex_i, Ey_i$  are the normal forces between columns in the x and y directions;

$Hx_i, Hy_i$  are the lateral shear forces between columns in the x and y directions;

$N_i, U_i$  are the normal effective forces and pore pressure at the base of the column;

$P_{vi}, Si$  are the external vertical forces and shear force mobilized at the base of the column;

$Xx_i, Xy_i$  are the vertical shear forces between columns in the plane perpendicular to the x and y directions.

By the Mohr-Coulomb resistance envelope criterion, the overall safety factor (FS) is defined (Cheng and Lau, 2008) as:

$$FS = \frac{S_{fi}}{S_i} = \frac{C_i}{S_i} + N'_i \tan \varphi_i \quad (4)$$

Where:

FS is the safety factor;

$S_{fi}$  is the net shear force available at the base of column i;

$N'_i$  is the effective normal force;

$C_i$  is the cohesion force, calculated by multiplying the cohesion of the soil at the base of the column by the area at the base of the column.

The components of the shear force S and the normal force N, at the base of column i, on the x, y and z axes are expressed as follows in Figure 3A, 3B, 3C and Equation 5 and Equation 6 as per Huang and Tsai (2000) and Huang, Tsai and Chen (2002):

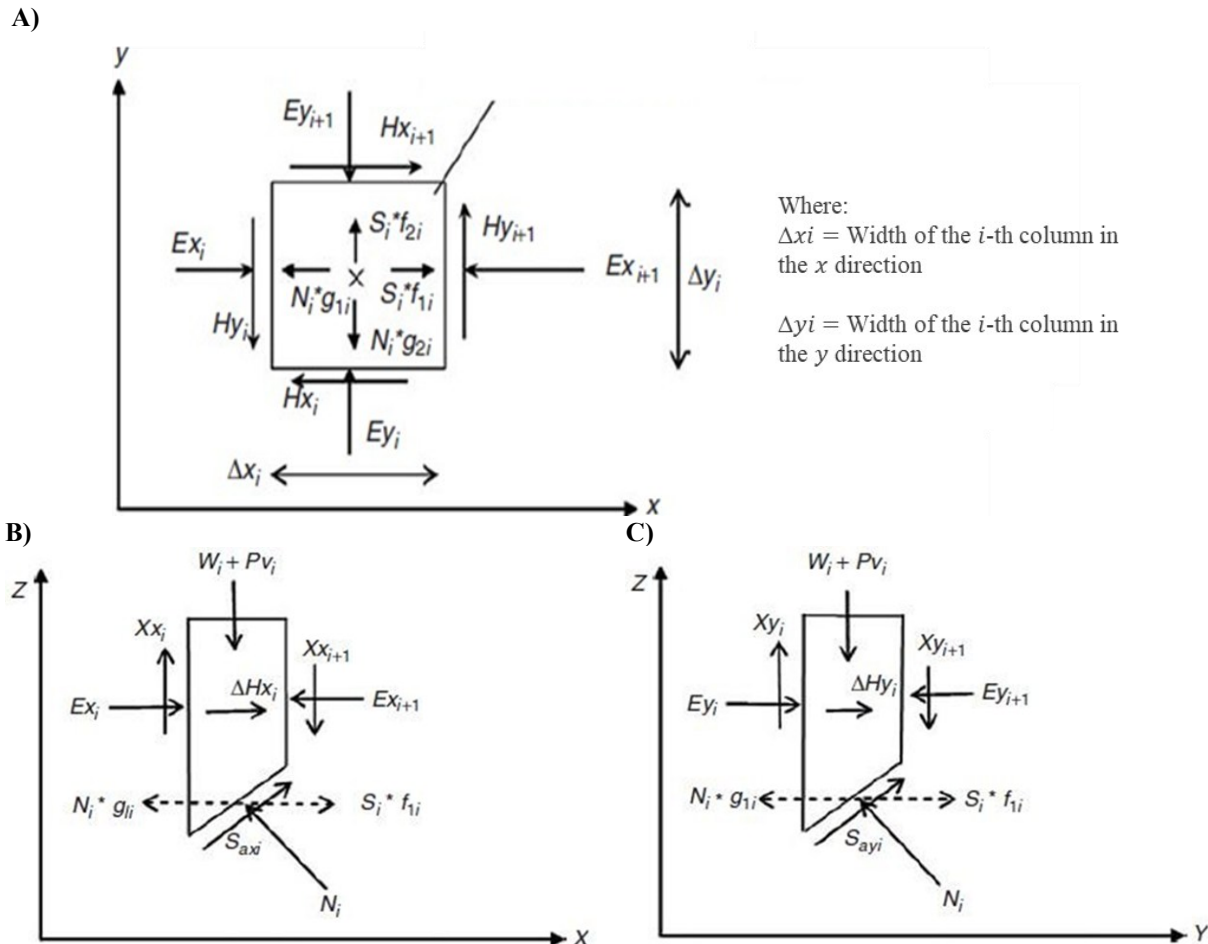


Figure 3 – (A) Balance of forces in the direction - XY of a typical column. (B) Equilibrium of horizontal forces in the -X direction of a typical column. (C) Equilibrium of horizontal forces in the -Y direction of a typical column.

Source: Chen and Lau (2008).

Where  $\{f_1 \times f_2 \times f_3\}$  and  $\{g_1 \times g_2 \times g_3\}$  are the unit vectors for  $S_i$  and  $N_i$ .

$$S_{xi} = f_1 \cdot S_i; S_{yi} = f_2 \cdot S_i; S_{zi} = f_3 \cdot S_i; \quad (5)$$

$$N_{xi} = g_1 \cdot N_i; N_{yi} = g_2 \cdot N_i; N_{zi} = g_3 \cdot N_i; \quad (6)$$

The commercial software "Slide3 Limit Equilibrium Analysis for Slopes" (Rocscience ®). it uses the general formulation of Cheng and Lau (2008), with some improvements implemented such as the use of several models of resistance envelopes (and not only Mohr-Coulomb).

There are still many limit equilibrium methods proposed in the literature by several authors and commonly used in slope stability projects. One of the most popular methods in limit equilibrium analyses is that it applies a more generalized formulation offering modeling in a more discrete manner than the method of Morgenstern and Price (1965) is the General Limit Equilibrium (GLE) method (Chugh, 1986). The method can be used for both force balancing and momentum balancing or, if necessary, only under force balancing conditions.

According to Gomes (2017), the GLE procedure consists of selecting an appropriate function that describes the variation of the angles of the forces between slices in order to achieve complete equilibrium, so computer programs are very sensitive and can generate numerical problems in the convergence of the failure that provides an accurate solution of the safety factor, (FS).

### 3. Case Study Description

#### 3.1 Location and Access Routes

The area of the Mineral Complex is located in the municipality of Patrocínio, Minas Gerais. The municipality is located in the region of Triângulo Mineiro and Alto Paranaíba. The route of the trip between the Capital of the State of Minas Gerais (Belo

Horizonte) and Patrocínio is about 417 km, made mainly through the BR-262, whose route continues in the direction of Ibiá by the MG-187, then by the MG-230 to Patrocínio, as shown in Figure 4.

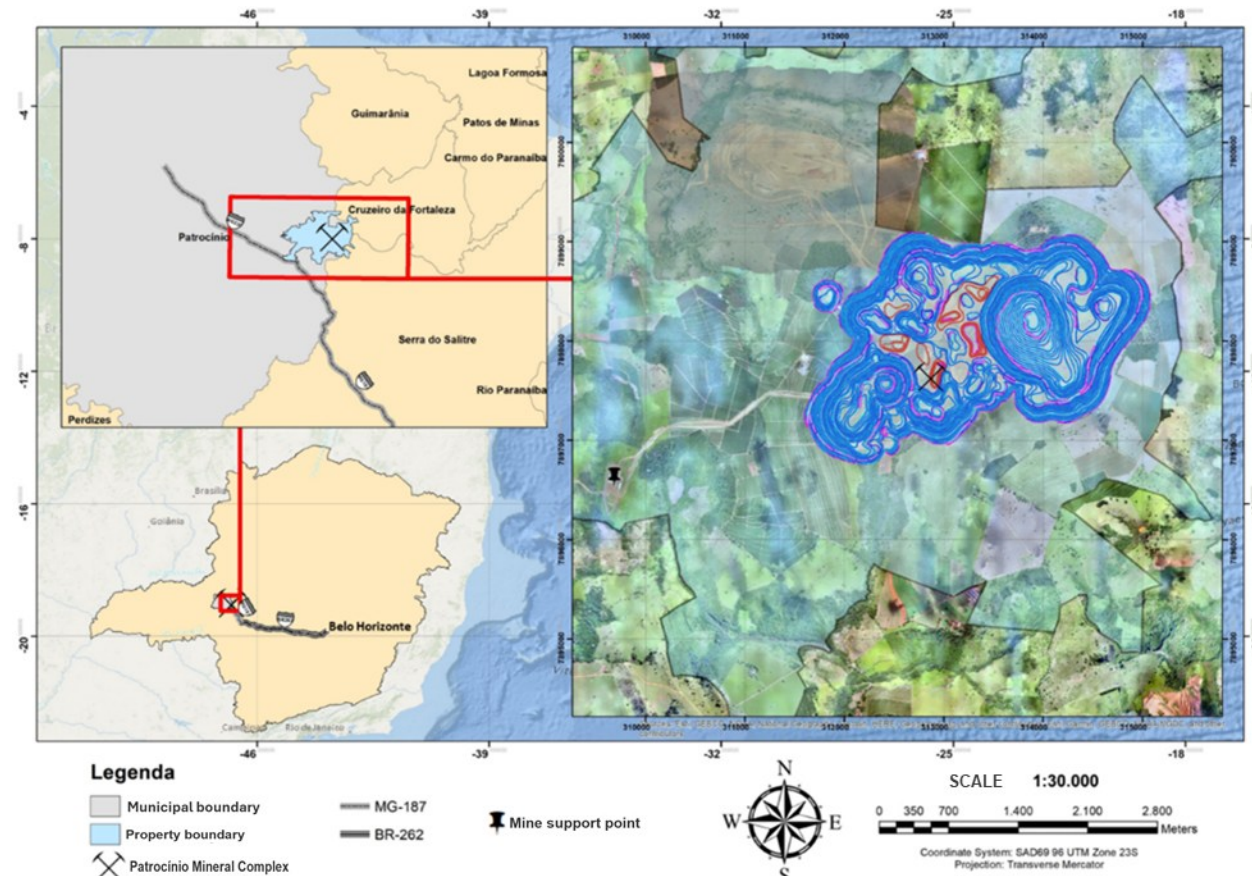


Figure 4 – Location: Patrocínio Mineral Complex - Studied Region.

Source: Prepared by the author with data extracted from the Word Ocean Reference ArcGIS Esri ®. Through bases made available by long-term planning (December 2023).

#### 4. Methodology

The methodology developed in this work encompasses slope stability analysis (AET) of the final pit, where the slopes reach more than 300 meters in height on an inclined terrain plane that limits the surface of a massif both in rock and soil.

In this research, the massifs of the final pit have a low geomechanical quality because they are essentially composed of soil massifs and saprolites. Although there are indications of structures in the saprolites such as faults and geological contacts, the available data do not provide information about their exact locations, nor their modeled geotechnical characteristics.

Given the previous reason, wedge, planar and tipping ruptures were not evaluated. Thus, the stability analyses were processed for asymmetric non-circular ruptures, performed using the commercial software Slide3 "Limit Equilibrium Analysis for Slopes" (Rocscience ®). Performed by iterative calculations through algorithms given the search option "Ellipsoid Surface and Spline Surface" the search methodology "Cuckoo search" with "Surface Altering Optimization".

To this end, the technique composed of the G.L.E./Morgenstern-Price method will be used, more consistent in terms of limit equilibrium (MEL) in two-dimensional and three-dimensional models, configuring the resistance parameters of the soil layers, governed by the Mohr-Coulomb envelope, considering the constitutive pattern for the eleven different types of soil and rock found in the research area.

Thus, knowing the advantages, limitations, and difficulties in the use of two-dimensional and three-dimensional models and according to the technical knowledge available about the massif so far, the following assumptions were adopted for the stability analyses:

- The analyses for asymmetric non-circular rupture for isotropic and heterogeneous materials, performed using Slide3 software "Limit Equilibrium Analysis for Slopes" (Rocscience ®).
- Minimum acceptable safety factor (FSmin) for Global slope scale = 1.2 – 1.3, with Low Failure Consequence (READ & STACEY, 2009).
- Adoption of material strength parameters based on existing laboratory tests and reports.
- Water table based on the drawdown surfaces for the final pit, according to the conceptual hydrogeological model elaborated.

---

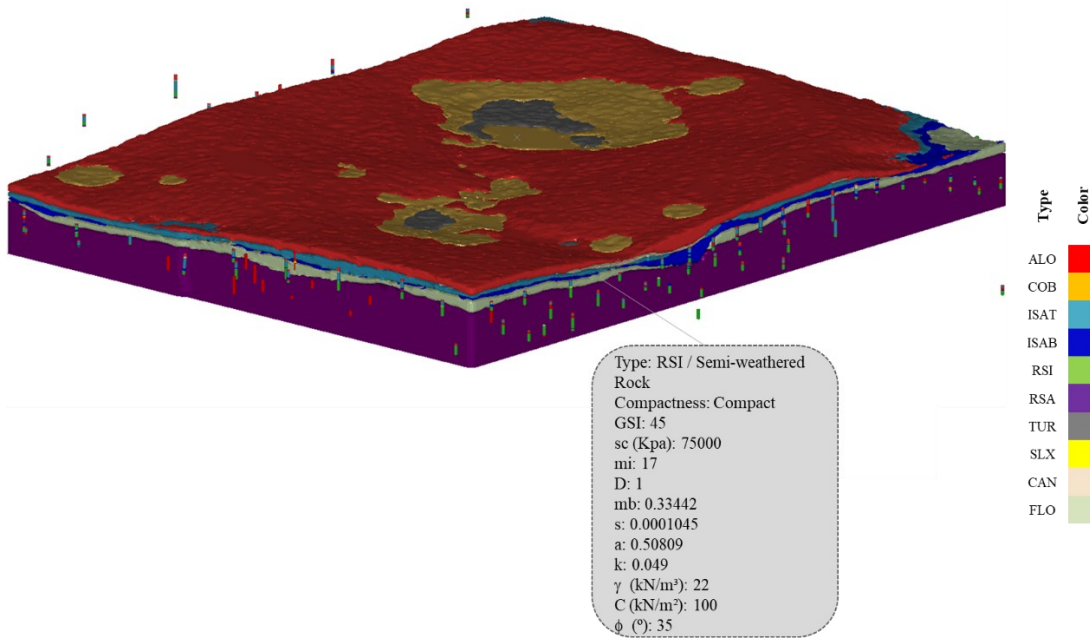
- Stability analysis considering drained slopes.

#### 4.1 Shear strength of soil layer

For the layers located inside the pit, the Mohr-Coulomb criterion was used, since this material is very weathered, behaving like a soil. The cohesion and friction angle were defined through the results of the triaxial compression tests provided by the mining company. Fast, pre-condensed, saturated, and neutral pressure triaxial compression tests (CIUsat) were performed with a series of four specimens per block and/or sampled material. The tests were carried out at confinement pressures of 100, 200, 400 and 800 kPa.  $c'\varphi$

The mine selected for the application of the proposed methodology already has a geological model prepared by the mining company's mining planning team, but only in block format. To carry out the analyses of the present research, it was necessary to convert the model to the format of solids, and thus be used as domains, lithological and weathering products. This conversion consisted of assigning "*Interior*" or "*Exterior*" attributes to the centroids of the blocks using Studio OP *Open Pit Design* DATAMINE ® software, command "*Create Isourfaces from Model – Wreframe*", for the lithological and weathering groupings as shown in Figure 5A and Figure 5B.

A)



B)

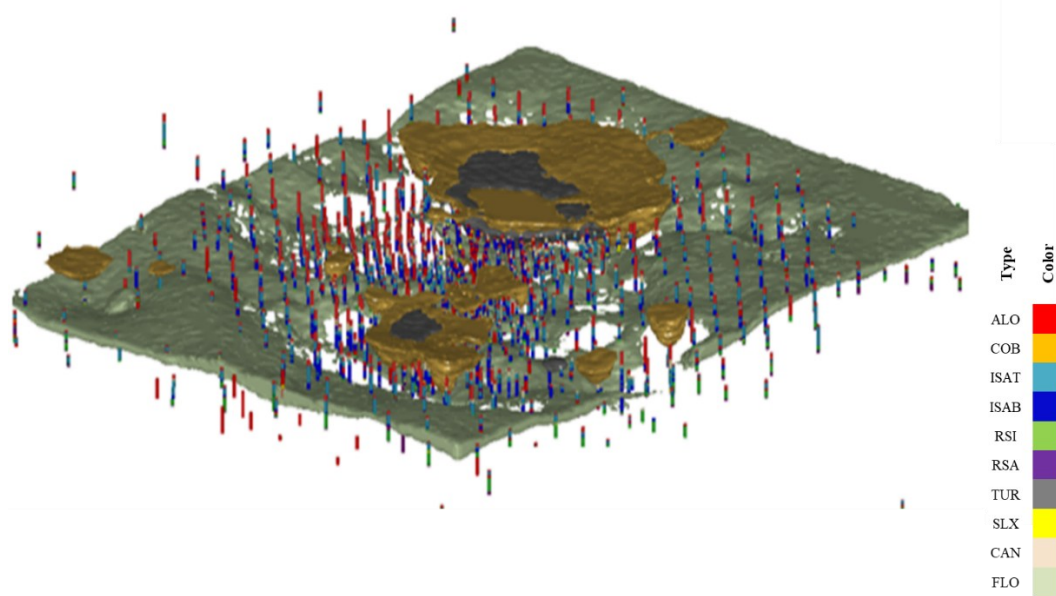


Figure 5 – (A) Geological model of blocks, lithological and weathering products. (B) Model of solids with lithological grouping according to geotechnical criteria.

Source: Prepared by the author – Studio OP Open Pit Design DATAMINE ®, through the Geological Model made available by Geologia de Longo Prazo (December 2023).

In order to support the slope stability analysis methodology, the water surface used in the 2D, and 3D analyses was obtained by the hydrogeological model and provided by the mining company. The hydrogeological model makes it possible to evaluate the hydraulic connections between the structures, as well as to provide the simulation of future scenarios to obtain estimates of the volume of water that should be managed. Delivering as the main product the geotechnics the current and final potentiometry, 3D potentiometric surface Figure 6, in order to identify the approximate position of the water level.

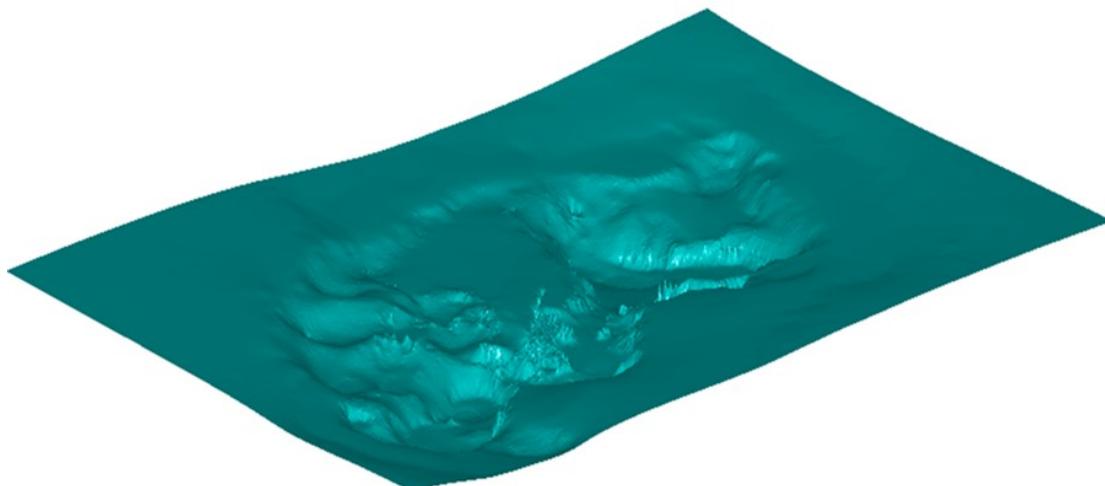


Figure 6 – 3D potentiometric surface.

Source: Prepared by the author – Studio OP Open Pit Design DATAMINE ®, through equipotentials made available by Geology and Hydrogeology - CMP (September 2023).

#### 4.2 2D and 3D Limit Equilibrium Stability Analysis

As it is a pit composed predominantly of friable lithotypes and materials without anisotropy, stability analyses were performed for ruptures initially of the type on a global scale, performed using the commercial software Slide3 "Limit Equilibrium Analysis for Slopes" (Rocscience ®). For the design of the solids of the 3D geological-geotechnical model of the final pit, to perform the stability analyses, the 3D geotechnical model was developed through the steps listed below:

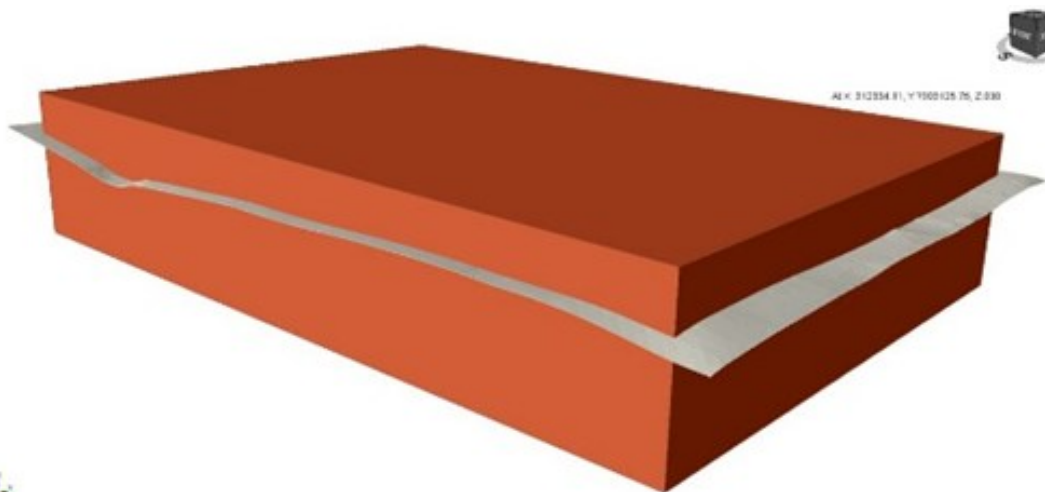
1. Definition of a volume of influence of the model through the creation of a contour based on the boundaries of the surfaces/shells referring to the materials (soil and rocks) received.
2. Creation of the solids and the mesh of the model by subdividing the volume of influence of its contour by means of the surfaces/shells received.
3. Assignment of geotechnical parameters in the numerical model.

#### 4.3 Model Outline Definition

With all the auxiliary surfaces/shells defined in Studio OP *Open Pit Design DATAMINE ®* software, the creation of the model in Slide3 "Limit Equilibrium Analysis for Slopes" (Rocscience ®) began. The surfaces were imported, creating a volume of influence of the model by creating a contour based on the boundaries of the closed surfaces of the solids referring to the materials of the final pit region.

It can be seen in Figure 7A and Figure 7B that the limits of the model, in red, were defined at the same depth (600.0 m) as the meshes received, with a height of up to 1,300.0 m without the need to keep much space left on the surface since the pit will be excavated.

A)



B)



Figure 7 – (A) - (B) Contour definition from the geometric surface imported into the 3D Slide.  
Source: Prepared by the author through the Slide 3D Rocscience ® software, (December 2023).

#### 4.4 Creation of the Solids

After defining the contour, it was possible to subdivide it into the solids of the model by means of the closed surfaces provided. The result is shown in Figure 8A. It is observed that the volume of the initial block was divided considering as limits all the imported surfaces referring to the lithotypes of the pit region. In this way, it was possible to identify each of the solids generated. For example, Figure 8B shows one of these solids, which so far does not have information on which lithotype it belongs to, which is a later step.

A)



B)

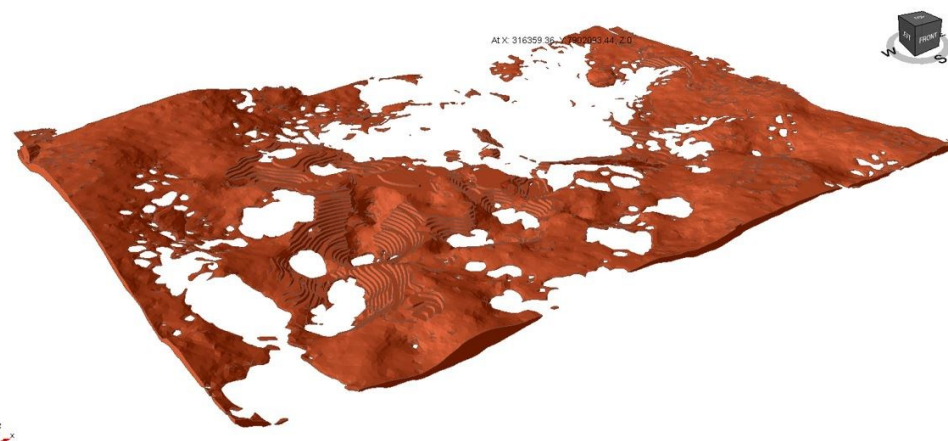


Figure 8 – (A) Division of the contour by means of the surfaces of the pit region. (B) Example of a volume separated from the other volumes after the contour has been divided before it is classified.

Source: Prepared by the author – Rocscience ® 3D Slide, (December 2023).

Thus, after applying the steps to all materials, the stage of creating the solids, also called mesh, is completed, having as a product a lithogemechanical model, still without geotechnical parameters applied.

#### 4.5 Assignment of Geotechnical Parameters to the Respective Solids

Figure 9 already shows in the different colors the assignment of the materials to the respective solids. The legend and the parameters applied are shown in Table 1.

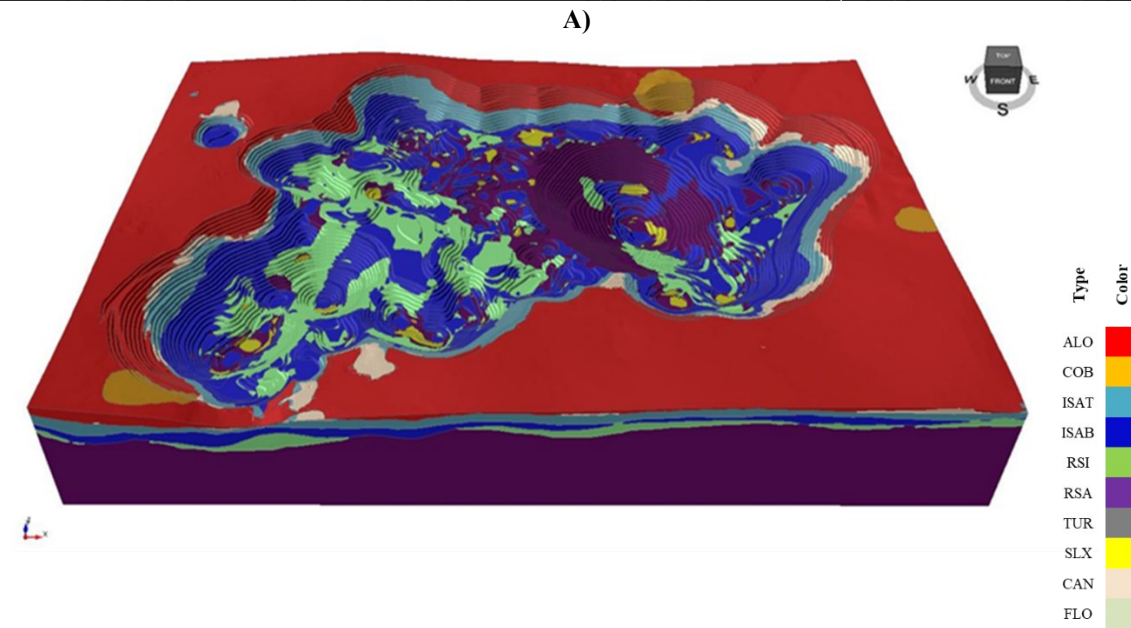


*Figure 9 – Complete lithogeomechanical model after the creation of all materials of interest.*  
Source: Prepared by the author – Rocscience ® 3D Slide, (December 2023).

Table 1 – Average geomechanical parameters used in the stability analysis.

| Parameters                         | Lithology  |          |          |          |         |           | Weathering  |          |              |              |  |
|------------------------------------|--|----------|----------|----------|---------|-----------|---|----------|--------------|--------------|--|
|                                    | TU<br>R  | CA<br>N  | FL<br>O  | SL<br>X  | AL<br>O | CO<br>B   | ISA<br>T  | IS<br>B  | RSI          | RSA          |  |
| Phy.<br>γ (kN/<br>m <sup>3</sup> ) | 13.<br>4   | 22.<br>5 | 21.<br>3 | 19.<br>5 | 14      | 14        | 19.<br>5  | 19.<br>7 | 22.5         | 22.5         |  |
| Hoek Brown<br>σγ (M<br>Pa)         | -  | -        | -        | -        | -       | -         | -   | -        | 75           | 155          |  |
| GSI                                | -  | -        | -        | -        | -       | -         | -   | -        | 40           | 56           |  |
| mi                                 | -  | -        | -        | -        | -       | -         | -   | -        | 17           | 17           |  |
| D                                  | -  | -        | -        | -        | -       | -         | -   | -        | 1            | 1            |  |
| Hoek Brown<br>mb                   | -  | -        | -        | -        | -       | -         | -   | -        | 0.234        | 0.7337       |  |
| s                                  | -  | -        | -        | -        | -       | -         | -   | -        | 4.54E<br>-05 | 0.0006<br>53 |  |
| the                                | -  | -        | -        | -        | -       | -         | -   | -        | 0.511<br>37  | 0.5037<br>7  |  |
| Mohr-<br>c<br>(kN/m <sup>2</sup> ) | 4  | 60       | 11       | 75       | 17      | 17        | 40  | 27       | 27           | 130          |  |
| ϕ (≡)                              | 27   | 35       | 21       | 37       | 30      | 30        | 33  | 36       | 32           | 36           |  |
| <b>Legenda</b>                     |  |          |          |          |         |           |   |          |              |              |  |
| γ                                  | material density in kN /m <sup>3</sup>                     |          |          |          |         | mb        | value of Hoek-Brown constant m for rock mass  |          |              |              |  |
| σc                                 | uniaxial elasticity strength of sound intact rock (MPa)    |          |          |          |         | "s" e "a" | constants of the Hoek-Brown failure criterion that depend on the characteristics of the rock mass |          |              |              |  |
| GSI                                | Geological Strength Index                                  |          |          |          |         | c         | cohesion (kN/m <sup>2</sup> )   |          |              |              |  |
| mi                                 | constants from the Hoek-Brown rupture draw for intact rock |          |          |          |         | ϕ         | friction angle (°)  |          |              |              |  |
| D                                  | damage factor due to detonation (dismantle by fire)        |          |          |          |         |           |   |          |              |              |  |

Source: Prepared by the author, based on the mine's available database (December 2023).

## 5. Results and Analysis

From the inserted three-dimensional model, the parameters of resistance of the soil layers have already been configured, thus governed by the Mohr-Coulomb envelope. Several deterministic stability analyses were performed so that the formulations of the methods could be satisfied by searching for asymmetric non-circular surfaces. In this way, concentrating the searches for the critical wedge, leaving the "free" software with the preset to find rupture surfaces throughout the three-dimensional model.

Generally, the process of searching for the critical slip surface involves trying different shapes, such as spheres and ellipsoids, to cut through the topography of the ground. The sliding mass above the cut is discretized into soil columns and its internal forces are resolved to static equilibrium to determine the factor of safety (FSmin). Scaled, rotated, and translated variations of these shapes are used to minimize the safety factor (FSmin) value obtained in the sliding mass.

Initially, the search option "Ellipsoid Surface" and the search methodology "Cuckoo search" with "Surface Altering Optimization" from the Slide3 software "Limit Equilibrium Analysis for Slopes" (Rocscience ®) were used. This makes it possible to determine the collapsible regions in terms of safety, highlighted through the surface safety map and contour data at least global, expressed through safety factor (FSmin).

The results of the 3D safety factor (FSmin) are presented in Table 2, and in Figure 9 the safety map as well as the legend with the global minimum factor.

To make the comparison between the 2D and 3D analyses more reliable, the cross-section used in the analyses was traced by the Slide3 software "Limit Equilibrium Analysis for Slopes" (Rocscience ®), which uses the general formulation of Chen and Yin (2007), with some improvements implemented, such as the use of several models of resistance envelopes and not only Mohr-

Coulomb. In this way, modeling errors, such as differences in geometry and geological layers, were eliminated or minimized.

Table 2 – Sliding Mass Discretization Results - Numerical Approaches (FS2D x FS3D) "Ellipsoid Surface".

| Dimension | Search Method | Surface Type | FS    | Maximum Columns X or Y -Slices | Maximum Interactions | Compute Priority (Highest) – Time(s) |
|-----------|---------------|--------------|-------|--------------------------------|----------------------|--------------------------------------|
| 2D        | Cuckoo serch  | Non-Circular | 1,222 | 50                             | 75                   | 28                                   |
| 3D        | Cuckoo serch  | Ellipsoid    | 1,373 | 50                             | 75                   | 428,136                              |

Source: Prepared by the author based on the results – Rocscience ® 3D Slide (December 2023).

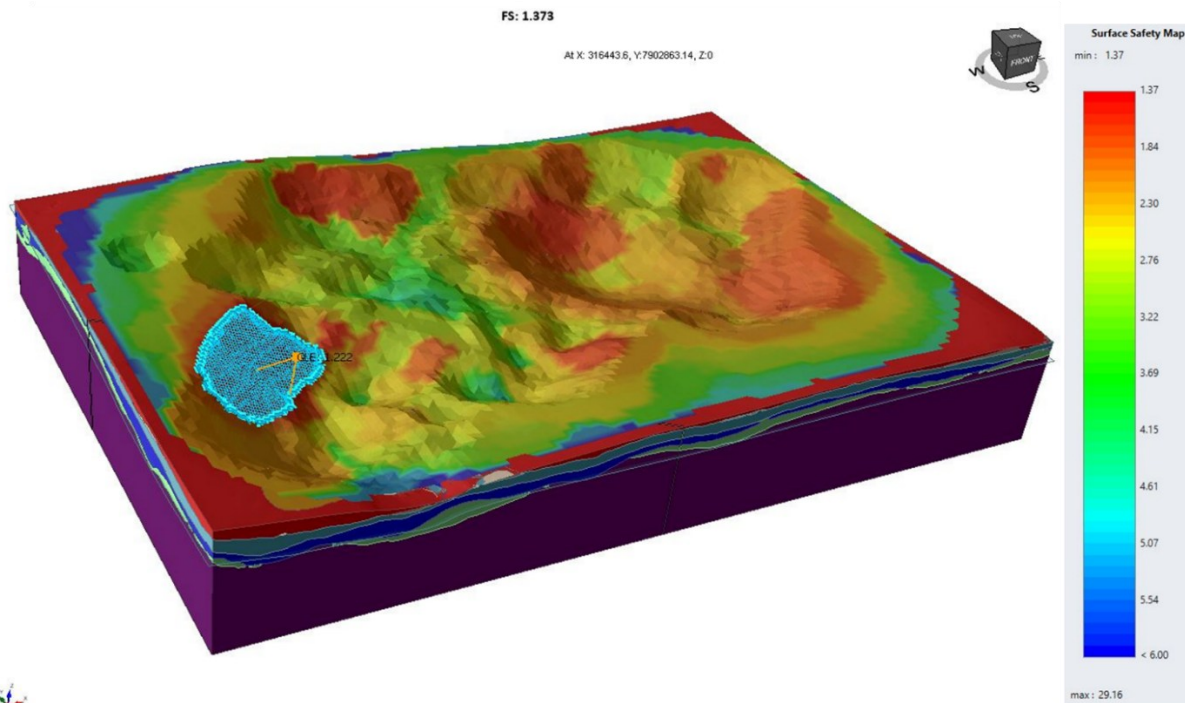


Figure 10 – (A) Surface safety map and contour data at minimum global (default). (B) 3D Rupture Surfaces, 2D Section – Final Pit "Ellipsoid Surface".

Source: Prepared by the author – Rocscience ® 3D Slide, (December 2023).

In the preliminary stability analysis, searches for the critical wedge were not concentrated, leaving the software "free" to find rupture surfaces throughout the three-dimensional model. In this way, it is possible to determine the collapsible regions in terms of safety, highlighted through the Map - surface safety and contour data at the global minimum. Also in Table 2, it can be observed that the safety factor in the case of the 3D model is higher than the 2D safety factor. It is known that the confinement effect of 3D rupture surfaces tends to result in higher safety factors than 2D analyses.

Comparing the values shown in Table 2, they indicate that the factors in the 3D model are 8% higher than in the 2D model. Despite this, the safety factors (SP) are satisfactory in relation to the minimum established in item 2.2.2 (FSmin = 1.2 – 1.3).

To concentrate the analyses to determine the critical rupture surface, enabling the study of the behavior, with the possibility of varying the number of Columns in X or Y - Slices until maximum convergence is obtained, numerous iterative calculations were performed through an exhaustive search in which all possible solutions are searched for a set of design variables. thus, representing the results in Table 3.

Table 3 – FS2D x FS3D Numerical Approaches - Maximum Number of Slices - Columns in X or Y "Ellipsoid Surface".

| Dimension | Search Method | Surface Type | FS             | Maximum Columns X or Y -Slices | Average | s     | C.V. (%) | Compute Priority (Highest) – Time(s) |
|-----------|---------------|--------------|----------------|--------------------------------|---------|-------|----------|--------------------------------------|
| 2D        | Cuckoo serch  | Non-Circular | 1,165<br>1,222 | 25<br>50                       | 1,226   | 0,059 | 4,830    | 29<br>28                             |

|    |                     |                  |  |       |     |       |       |       |          |
|----|---------------------|------------------|--|-------|-----|-------|-------|-------|----------|
|    |                     |                  |  | 1,289 | 100 |       |       |       | 31       |
|    |                     |                  |  | 1,196 | 150 |       |       |       | 57       |
|    |                     |                  |  | 1,185 | 200 |       |       |       | 64       |
|    |                     |                  |  | 1,177 | 250 |       |       |       | 75       |
|    |                     |                  |  | 1,303 | 300 |       |       |       | 82       |
|    |                     |                  |  | -     | 350 |       |       |       | -        |
|    |                     |                  |  | 1,260 | 25  |       |       |       | 237,19   |
|    |                     |                  |  | 1,373 | 50  |       |       |       | 428,136  |
|    |                     |                  |  | 1,322 | 100 |       |       |       | 1167,73  |
|    |                     |                  |  | 1,269 | 150 |       |       |       | 4103,95  |
|    |                     |                  |  | 1,389 | 200 |       |       |       | 5004,51  |
|    |                     |                  |  | 1,252 | 250 |       |       |       | 14010,64 |
|    |                     |                  |  | 1,352 | 300 |       |       |       | 26801,18 |
|    |                     |                  |  | -     | 350 |       |       |       | -        |
| 3D | <i>Cuckoo serch</i> | <i>Ellipsoid</i> |  |       |     | 1,317 | 0,052 | 3,982 |          |

Source: Prepared by the author based on the results – Rocscience ® 3D Slide (December 2023).

### 5.1 Optimization of computational numerical analysis

All surfaces generated in the previous results are ellipsoidal. According to Ma et al. (2022), slip surfaces are rarely ellipsoidal or spherical, ellipsoidal search alone may not always produce the true minimum safety factor (FSmin) on a slope.

Spline search is a powerful feature of the Slide3 software "Limit Equilibrium Analysis for Slopes" (Rocscience ®) and recently updated for use in the software, where using 3D spline-based surfaces, which are varied to determine the critical slip surface, is generally more effective at predicting the minimum safety factor (FSmin) than ellipsoidal or spherical survey (ROSCIENCE, 2022).

To better predict the true minimum safety factor (FSmin) for the slopes of the final pit, a combination of the more powerful "Spline Surface" methods and the "*Cuckoo serch*" search methodology with "*Surface Altering Optimization*" was then employed incrementally.

Like the previous analyses, the maximum convergence was also achieved through an exhaustive search in which all possible solutions are searched for a set of design variables, so Table 4 shows through the analyses the results, the numerical approaches, and the minimum safety factor (FSmin) 2D and 3D together with the average results of the minimum safety factor (FSmin) 2D and 3D.

Table 4 – FS2D x FS3D Numerical Approaches - Maximum Number of Slices - Columns in X or Y "Spline Surface".

| Dimension | Search Method       | Surface Type        | FS    | Maximum Columns X or Y -Slices | Average | s     | C.V. (%) | Compute Priority (Highest) – Time(s) |
|-----------|---------------------|---------------------|-------|--------------------------------|---------|-------|----------|--------------------------------------|
| 2D        | <i>Cuckoo serch</i> | <i>Non-Circular</i> | 1,235 | 25                             | 1,223   | 0,060 | 4,939    | 25                                   |
|           |                     |                     | 1,269 | 50                             |         |       |          | 40                                   |
|           |                     |                     | 1,298 | 100                            |         |       |          | 52                                   |
|           |                     |                     | 1,136 | 150                            |         |       |          | 73                                   |
|           |                     |                     | 1,181 | 200                            |         |       |          | 86                                   |
|           |                     |                     | 1,158 | 250                            |         |       |          | 93                                   |
|           |                     |                     | 1,257 | 300                            |         |       |          | 140                                  |
|           |                     |                     | -     | 350                            |         |       |          | -                                    |
| 3D        | <i>Cuckoo serch</i> | <i>Spline</i>       | 1,387 | 25                             | 1,322   | 0,062 | 4,726    | 123,10                               |
|           |                     |                     | 1,346 | 50                             |         |       |          | 690,71                               |
|           |                     |                     | 1,398 | 100                            |         |       |          | 1424,14                              |
|           |                     |                     | 1,278 | 150                            |         |       |          | 3684,65                              |
|           |                     |                     | 1,279 | 200                            |         |       |          | 9736,35                              |
|           |                     |                     | 1,213 | 250                            |         |       |          | 11309,52                             |
|           |                     |                     | 1,355 | 300                            |         |       |          | 14819,25                             |
|           |                     |                     | -     | 350                            |         |       |          | -                                    |

Source: Prepared by the author based on the results – Rocscience ® 3D Slide (December 2023).

Figure 11 shows the graph, in which the results of the 2D and 3D safety factors for the deterministic analyses are plotted, corresponding to each scenario of variation of the X or Y Columns - Slices, both for the "*Ellipsoid*" surface type and for the

### Spline surface.

The results plotted in the graph indicate a variation in the results of the 2D and 3D safety factors as the number of slices and/or columns increases. This is due to the geometric constraint imposed on the software's search for rupture wedges.

The more 2D slices or 3D columns are incorporated into the searches, the more the software is free to search for rupture wedges with different geometries, and with each round of analysis an entirely new search, which will not necessarily return the same results as wedges with different numbers of columns and/or slices. The more columns and/or slices are increased, the more the geometric precision of the rupture wedges increases, allowing the software to search for different and more precise geometries, following the geological contact or even the external geometry of the massif or slope.

By indicating 50x50 columns, the Slide 3 software will frame the breaking surface within a column grid composed of 50 columns horizontally and 50 columns vertically, totaling 2500 columns. The critical rupture surface will always be framed within this mesh, where the width of the column base will vary as a function of the size of the critical rupture surface. By varying the number of columns in a search for a rupture wedge, the searches for critical rupture wedges are refined, making it possible to find wedges with a lower safety factor (FSmin), even spatially in different places.

The stability analysis corresponding to 300x Columns in X or Y - Slices, represents the maximum convergence, precisely because of the excessive number of columns in relatively small wedges. Thus, there was no further change in the values of the 2D and 3D safety factor factors (FSmin) with the addition of X or Y Columns - Slices.

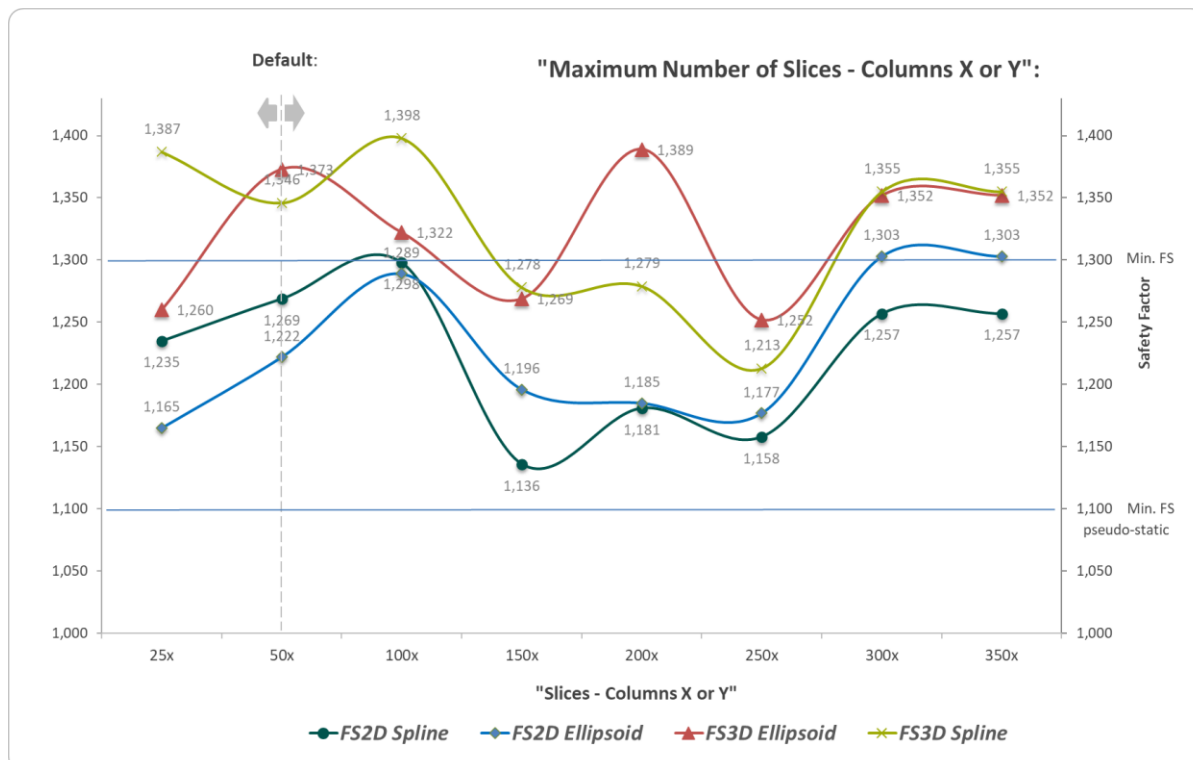


*Figure 11 – Numerical Approaches (FS2D x FS3D) - Maximum Number of Columns in X or Y - Slices.*  
Source: Prepared by the author based on the results of the Numerical Approaches – Rocscience ® 3D Slide (December 2023).

The confinement effect of 3D rupture surfaces tends to result in higher safety factors than 2D analyses, with the exception of geotechnical problems that have purely 3D behaviour where 2D analyses cannot replicate. The variation of the number of Columns in X or Y - Slices until maximum convergence is obtained, results in different values of 2D and 3D factor of safety (FSmin), and critical rupture surface geometry spatially in different places, even reducing the computational effort and the three-dimensional numerical model using search limits.

It is noted that the variations of the 2D and 3D factor of safety factors (FSmin) have a high coefficient of variation compared to the increase in the number of Columns in X or Y - Slices, sometimes for larger, sometimes for smaller values. The determination of the ideal number of columns depends on the size of the rupture wedges and the geological complexity of the mass, and not necessarily the increase in the number of columns leads to lower safety factors (FSmin), as occurs in finite element analyses.

The numerical approach (FS2D x FS3D), medium safety factor (FSmin) using "Spline Surface", is slightly lower than the numerical approach (FS2D x FS3D), using the average safety factor (FSmin) "Ellipsoid Surface". Despite this, the minimum mean 2D and 3D safety factor (FSmin) for both approaches are satisfactory in relation to the minimum established in item 2.2.2 for the Global slope scale = 1.2 – 1.3, with Low Failure Consequence. The result of the safety factor (FSmin) corresponding to the pseudo-static 3D model and higher with respect to the pseudo-static 2D model, and only the safety factor (FSmin)

corresponding to the 3D model are satisfactory in relation to the minimum established in item 2.2.2 (FSmin = 1.10).

## 6. Final Thoughts

The main objective of this work was to investigate the influence of two- and three-dimensional effects on the occurrence of displacements, and on the variation of safety factors against slope failure during the process of variations in the number of columns and slices, alternating the methodology of searching for the critical slip surface.

The three-dimensional geotechnical model was made according to the data provided by the

while the materials were geotechnically characterized through laboratory tests and the existing database.

For the present case study, together with work carried out in the project of this same project, it was sought to evaluate the safety factors (FSmin), reliability of the different requests, and compare them with references of national and international standards that provide for mining pits, since there is still no knowledge of regulation for results for safety factors (FSmin) given through 3D models.

In the evaluation of the two-dimensional and three-dimensional stability condition, the results indicated the following main points:

With the average strength parameters of the materials, the 2D safety factor (FSmin) was 1.22 and the 3D safety factor (FSmin) was 1.32 on the Global slope scale = 1.2 – 1.3, with Low Failure Consequences, recommended by several authors for pit slopes. Enough to define an unstable slope condition.

When comparing numerical approach (FS2D vs. FS3D), we can see that the 3D results are about 8% higher. This comparison allows us to validate the results.

Still for the present case study, some conclusions can be made:

1. The safety factors calculated in 3D models are usually slightly higher than the corresponding values estimated in 2D models. The use of 2D analyses is simpler to operate, and 3D models are not necessary, which explains the predominance of 2D analyses in geotechnical engineering, given the difficulty in producing reliable 3D models.

2. Varying the number of X or Y-Slice Columns to achieve maximum convergence results in different values of safety factor (FSmin) and critical breaking surface geometry spatially in different locations.

## Thanks

The authors would like to thank the support of the Graduate Program in Mining Engineering of the Federal Center for Technological Education of Minas Gerais for the development of this research.

## References

ALBATAINEH, N. Slope Stability Analysis Using 2D and 3D Methods. Akron, 2006. 129 p. master's thesis, University of Akron, 2006.

ANAGNOSTI, P. Three-Dimensional Stability of Fill Dams. Proceedings of the 7th International Conference on Soil Mechanics and Foundation Engineering, v. 02, p 275 – 280, 1969.

ANTOCHEVIZ, R. B. Methodology for Determining the Procedure to be Used in a Slope Stability Analysis – Circular Rupture. Porto Alegre, 2018. 98 p. Dissertation (master's degree in mining engineering) – PPGEM of the Federal University of Rio Grande do Sul.

AZZOUZ, A. S.; BALIGH, M. M. Loaded Areas on Cohesive Slopes. ASCE Journal of the Geotechnical Engineering Division, v. 109, n. GT 05, p. 724 – 729, 1983.

BALIGH, M. M.; AZZOUZ, A. S. End Effects on the Stability of Cohesive Slopes. ASCE Journal of the Geotechnical Engineering Division, v. 101, n. GT 11, p. 1105 – 1117, 1975.

BISHOP, A. W. The Use of Slip Circle in the Stability Analysis of Earth Slopes. Géotechnique, v. 05, n. 01, p. 7 – 17, 1955.

BRETAS, T. C. Three-dimensional probabilistic retroanalysis by equilibrium-limit of slope ruptures in Belo Horizonte/MG. Ouro Preto, 2020. Dissertation (master's degree in Geotechnics) – Federal University of Ouro Preto. School of Mines. Geotechnics Nucleus.

CAPELLI, R. B. Analytical Methodologies and Numerical Modeling for the Optimization of Mining Slope Slopes on a Profit Basis. Ouro Preto, 2018. 15 p. Dissertation (master's degree in Geotechnics) – Federal University of Ouro Preto. School of Mines. Geotechnics Nucleus.

CAVOUNIDIS, S.; KALOGEROPOULOS, H. End Effects on the Stability of Cuts in Normally Consolidated Clays. Revista Italiana di Geotechnica, v. 02, p. 85 – 93, 1992.

---

CHEN, R. H. Three-Dimensional Slope Stability Analysis. Joint Highway Research Project, Eng. Experiment Station, Purdue University, Report JHRP-81-17, 1981.

CHEN, R. H.; CHAMEAU, J. L. Three-Dimensional Limit Equilibrium Analysis of Slopes. *Géotechnique*, v. 32, n. 01, p. 31 – 40, 1982.

CHENG, Y. M.; YIP, C. J. Three-Dimensional Asymmetrical Slope Stability Analysis Extension of Bishop's, Janbu's, and Morgenstern-Price's Techniques. *Journal of Geotechnical and Geoenvironmental Engineering*, v. 133, n. 12, p. 1544 – 1555, Dec. 2007.

COSTA, E. A. Assessment of Geotechnical Threats and Risks Applied to Slope Stability. Porto Alegre, 2005. 20 p. Dissertation (master's degree in civil engineering) – Federal University of Rio Grande do Sul.

FELLENIUS, W. "Calculations of the stability of earth dams". In: *Trans. 2nd Congr. Large Dams*. Washington, v. 4, pp. 445-463, 1936.

FREDLUND, MD.; LU, H.-H.; MYHRE, T.; MERCER, K. Open Pit 3D Limit Equilibrium Numerical Modelling of Complex Geostructures. *Slope Stability*, African Institute of Mining and Metallurgy, 2015.

GENS, A.; HUTCHINSON, J.; CAVOUNIDIS, S. Three-Dimensional Analysis of Slides in Cohesive Soils, *Géotechnique*, v. 38, n. 01, p. 1 – 23, 1988.

HOVLAND, H. J. Three-Dimensional Slope Stability Analysis Method. *ASCE Journal of the Geotechnical Engineering Division*, v. 103, n. GT 09, p. 971 – 986, 1977.

HUANG, C.-C.; TSAI, C.-C. New method for 3D and asymmetrical slope stability analysis. *Journal of Geotechnical and Geoenvironmental Engineering*, v. 126, n. 10, p. 917 – 927, Oct. 2000.

HUANG, C.-C.; TSAI, C.-C.; CHEN, Y.-H. Generalized Method for Three-Dimensional Slope Stability Analysis. *Journal of Geotechnical and Geoenvironmental Engineering*, v. 128, n. 10, p. 836–848, out. 2002.

HUNGR, O. An Extension of Bishop's Simplified Method of Slope Stability Analysis to Three Dimensions. *Géotechnique*, v. 37, n. 1, p. 113 – 117, 1987.

HUNGR, O.; SALGADO, F. M.; BYRNE, P. M. Evaluation of a Three-Dimensional Method of Slope Stability Analysis. *Canadian Geotechnical Journal*, v. 26, p. 679–686, 1989.

JANBU, N. Slope Stability Computations. In: HIRCHFELD, R. C.; POULOS, S. J. (Eds) *Embankment- Dam Engineering*, New York: John Wiley & Sons, 1973. p. 47 – 86.

KALATEHJARI, R.; THERE, NAZRI. A Review of Three-Dimensional Slope Stability Analyses based on Limit Equilibrium Method. *The Electronic Journal of Geotechnical Engineering*, v. 18, p. 119–134, jan. 2013.

LAM, L.; FREDLUND, D.G. A General Limit Equilibrium Model for Three-dimensional Slope Stability Analysis, *Canadian Geotechnical Journal*, NRC Research Press, v. 30(6), p. 905–919, Dec. 1993.

LESHCHINSKY, D.; BAKER, R. Three-Dimensional Stability: End Effects. *Japanese Society of Soil Mechanics and Foundation Engineering*, v. 26, n. 4, p. 98 – 110, Dec. 1986

LU, H.-H.; FREDLUND, MD.; FREDLUND, DG. Three-dimensional limit equilibrium analysis of open pits, in PM Dight (ed.), *Proceedings of the International Symposium on Slope Stability in Open Pit Mining and Civil Engineering*, Australian Centre for Geomechanics, Perth, p. 541 – 554, 2013.

MONTGOMERY, D.C.; RUNGER, G. C. *Applied Statistics and Probability for Engineers*. Rio de Janeiro, 2003. 4th ed: translated by Verônica Calado; LTC.

OLIVEIRA, D. M. A. Three-Dimensional Stability Analysis and Sensitivity Study of the Conditioning Parameters of the Rupture of a Hollow Slope. Ouro Preto, 2020. Dissertation (master's degree in Geotechnics) – Federal University of Ouro Preto. School of Mines. Geotechnics Nucleus.

READ, J., STACEY, P. *Guidelines for Open Pit Sole Design*. Australia: CSIRO PUBLISHING, 2009.

ROCSCIENCE. (2022). Slide3 – 3D Limit Equilibrium Slope Stability Overview. Available at: <https://www.rocscience.com/help/slide3/tutorials/2d-extruded-models/slope-with-water-table>. Accessed on: Mar 23, 2022.

SPENCER, E. A. Method of Analysis of the Stability of Embankments Assuming Parallel Inter-Slice Forces. *Géotechnique*, v.

---

17, n. 1, p. 11 – 26, 1967.

TREVIZOLLI, M.; FREDLUND, M.; LU, H. Column Resolution Impacts on 3D Open Pit Stability, nov. 2021.

YAMAGAMI, T.; JIANG, C. J. A Search for the Critical Slip Surface in Three-Dimensional Slope Stability Analysis. *Soils and Foundations*, v. 37, n.3, p. 1 – 16, 1997.

ZHENG, H. Eigenvalue Problem from the Stability Analysis of Slopes. *Journal of Geotechnical and Geoenvironmental*

ZHENG, H. Eigenvalue Problem from the Stability Analysis of Slopes. *Journal of Geotechnical and Geoenvironmental Engineering*, v. 135, n. 5, p. 647 – 656, 2009.

ZHOU, X. P.; CHENG, H. Analysis of Stability of Three-Dimensional Slopes Using the Rigorous Limit Equilibrium Method. *Engineering Geology*, v. 160, p. 21 – 33, 2013.